Influence of neutron-core excitations on high-spin states in ^{88}Sr

E. A. Stefanova,[1,2] R. Schwengner,[1] J. Reif,[1,*] H. Schnare,[1,†] F. Dönau,[1] M. Wilhelm,[3] A. Fitzler,[3] S. Kasemann,[3] P. von Brentano,[3] and W. Andrejtscheff[1,2]

[1]*Institut für Kern- und Hadronenphysik, Forschungszentrum Rossendorf, D-01314 Dresden, Germany*

[2]*Institute for Nuclear Research and Nuclear Energy, BAS, 1784 Sofia, Bulgaria*

[3]*Institut für Kernphysik, Universität zu Köln, D-50937 Köln, Germany*

(Received 4 July 2000; published 13 October 2000)

High-spin states of the nucleus ^{88}Sr have been studied via the reaction ^{80}Se(^{11}B,$p2n$) at a beam energy of 45 MeV. Gamma rays were detected with the six-detector array OSIRIS CUBE. The level scheme of ^{88}Sr has been extended up to $E\approx 11$ MeV and $J=17$. Mean lifetimes of three levels have been determined using the Doppler-shift-attenuation method. The level structures in ^{88}Sr have been interpreted in terms of the shell model. The calculations were performed in the configuration space $(0f_{5/2},1p_{3/2},1p_{1/2},0g_{9/2})$ for the protons and $(1p_{1/2},0g_{9/2},1d_{5/2})$ for the neutrons. These calculations describe the high-spin level sequences linked by $M1$ transitions with strengths of $B(M1)\approx 0.3$ to 1.4 W.u. as multiplets of seniority $v=4$ and 6 states including proton configurations and neutron-core excitations.

PACS number(s): 23.20.Lv, 25.85.Ge, 27.50.+e

I. INTRODUCTION

In our investigations of $N=48$, 49, and 50 nuclei, a variety of structural phenomena has been observed. The yrast sequences of the $N=48$ nuclei ^{83}Br, ^{85}Rb, and ^{87}Y display moderate collective $E2$ transition strengths of $B(E2)\approx 15$ Weisskopf units (W.u.) up to $J^{\pi}=17/2^{+}$, while at higher spin positive-parity as well as negative-parity states form multipletlike $\Delta J=1$ sequences including strong $M1$ transition strengths of up to $B(M1)\approx 1$ W.u. [1–4]. In shell-model calculations using the model space $\pi(0f_{5/2},1p_{3/2},1p_{1/2},0g_{9/2})$ $\nu(0g_{9/2},1p_{1/2})$, the collective properties of the $9/2^{+},13/2^{+},17/2^{+}$ states result from a coherent superposition of many contributing components including $\pi(fp)$ and $\nu(0g_{9/2}^{-2})$ excitations. The high-spin states with $21/2\leqslant J\leqslant 33/2$ are described as members of seniority $v=3$ and $v=5$ multiplets arising from a recoupling of the spins of the involved proton and neutron orbitals. This recoupling generates the large $B(M1)$ values. The low-spin states of the $N=49$ nuclei ^{85}Kr and ^{86}Rb are characterized by proton excitations coupled to the unpaired $g_{9/2}$ neutron [5,6]. At higher spins ($J\geqslant 15$), however, evidence for neutron particle-hole excitations across the $N=50$ shell gap has been found [6]. Analogously, we observed high-spin states in the $N=50$ nuclei ^{86}Kr and ^{89}Y which cannot be explained by pure proton configurations. For their description, the breakup of the closed neutron shell and the excitation of one neutron across the shell gap into the $1d_{5/2}$ orbital is important [5,7,8].

To extend our knowledge on the nuclear structure of $N=50$ nuclei, we have studied the nucleus ^{88}Sr where the number of protons is at the subshell closure $Z=38$. For the $2_1^{+}\rightarrow 0_1^{+}$ transition in ^{88}Sr a value of $B(E2)=7.20(22)$ W.u. was adopted in Ref. [9] on the basis of the results obtained in Refs. [10,11]. Similarly low values of $B(E2)\approx 8$ W.u. and 13 W.u. were obtained for the $2_1^{+}\rightarrow 0_1^{+}$ transitions in the chain of $^{90-94}$Sr and ^{96}Sr, respectively [12]. In this way, the nuclei $^{88-96}$Sr as well as $^{90-98}$Zr appear to form the region of lowest collectivity of known nuclides heavier than ^{56}Ni except for the spherical Pb isotopes [12].

High-spin states of ^{88}Sr were previously studied using the ^{86}Kr(α,$2n\gamma$) reaction [13] up to about 5.6 MeV. In the ^{87}Sr(d,p) studies [14–17], the broken-core $\nu(0g_{9/2}^{-1}1d_{5/2}^{1})$ configuration is found to dominate the first $(6)^{+}$ and $(7)^{+}$ states which were found to be part of the high-spin level

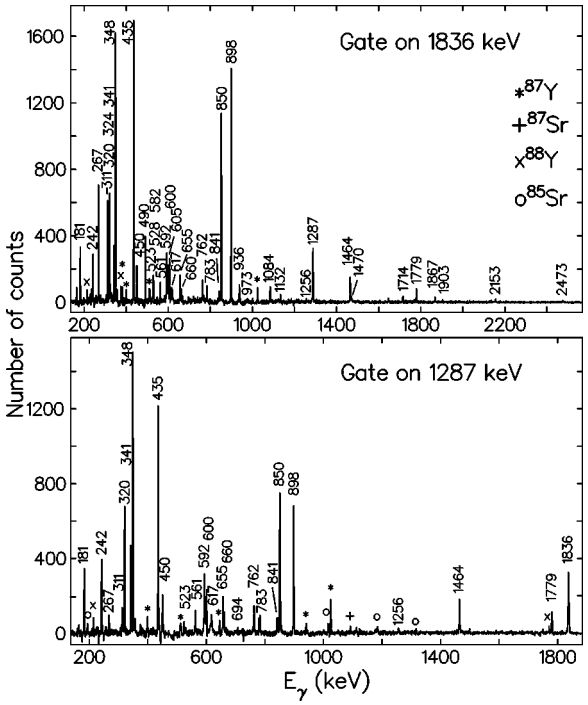

FIG. 1. Examples of background-corrected coincidence spectra. Peaks labeled with their energy are assigned to ^{88}Sr.

*Present address: Heyde+Partner, D-01099 Dresden, Germany.

†Present address: Deutsches Institut für Medizinische Dokumentation und Information, D-50899 Köln, Germany.

 ©2000 The American Physical Society

scheme in a recent heavy-ion-induced fission experiment [18]. In Ref. [18], the level scheme was extended up to 8.4 MeV but spin assignments to the new levels could not be made. In the present work, we have extended the level scheme up to $E \approx 11.4$ MeV and $J = 17$. We have established a new sequence of $M1$ transitions built on top of the 8335 keV level and made spin assignments for all levels.

II. EXPERIMENTAL METHODS AND RESULTS

Excited states of ^{88}Sr were populated via the reaction ^{80}Se(^{11}B,$p2n$) at a beam energy of 45 MeV. The ^{11}B beam was delivered by the FN tandem accelerator of the University of Cologne. The target consisted of a 2.3 mg cm^{-2} thick layer of ^{80}Se enriched to 99.1% on a gold backing of thickness 2.5 mg cm^{-2}. Gamma rays were detected with the six-detector array OSIRIS CUBE [19]. Singles spectra and γ-γ coincidences were recorded in parallel with the Cologne FERA analyzer [20]. A total of 3×10^8 prompt γ-γ coincidence events were collected and sorted off-line into E_γ-E_γ matrices for either all or selected detector combinations. Coincidence spectra were extracted by setting gates on certain peak and background intervals in the E_γ-E_γ matrices using the codes ESCL8R [21] and VS [22].

In Fig. 1, examples of background-corrected coincidence spectra are shown which were extracted from the total matrix including all detector combinations and used to construct the level scheme of ^{88}Sr. The γ rays assigned to ^{88}Sr on the basis of the present experiment are listed in Table I.

A. Gamma-gamma directional correlations

The analysis of directional correlations of coincident γ rays emitted from oriented states (DCO) provides information on the multipole order of the transitions and, thus, can be used to assign spins to the emitting states. This method is described in Refs. [23–25]. The DCO ratio is defined as $R_{\mathrm{DCO}} = Y(\theta_1, \theta_2, \Phi)/Y(\theta_2, \theta_1, \Phi)$, where the quantity $Y(\theta_1, \theta_2, \Phi)$ is the coincidence intensity of a transition γ_2 measured at the angle θ_2 relative to the beam by gating with a transition γ_1 measured at the angle θ_1. The quantity Φ is the opening angle between the two planes opened by the

TABLE I. Gamma rays assigned to ^{88}Sr in the present experiment.

E_γ [a] (keV)	I_γ [b]	R_{DCO} [c]	$\sigma\lambda$ [d]	J_i^π	J_f^π	E_i (keV)
181.4	8.4(4)	0.65(10)	$M1$	$13^{(+)}$	$12^{(+)}$	8274.4
241.6	6.9(6)	1.15(22)	$M1$	$12^{(+)}$	$12^{(+)}$	8334.7
266.9	12.3(4) [f]	0.71(6) [h]	$M1$	$11^{(-)}$	$10^{(-)}$	7908.1
267.1	6.1(2) [f]				7^+	5369.4
311.3	17.4(7)	0.72(8)	$M1$	$10^{(-)}$	$9^{(-)}$	7640.7
319.6	16.1(4) [f]	0.60(4) [h]	$M1$	$12^{(+)}$	$11^{(+)}$	8093.0
319.6	5.5(2) [f]		$(M1)$	7	7^-	4686.6
324.2	2.8(2)	0.47(18)	$(E1)$	8	7^+	5426.5
340.5	9.3(4)	0.54(6)	$M1$	$11^{(+)}$	10^+	7773.4
348.3	49(1)	0.68(3)	$M1$	7^-	6^-	4367.0
434.6	58(1)	0.83(4)	$M1/E2$	6^-	5^-	4018.7
449.6	9.4(5)	0.64(11)	$M1$	$15^{(+)}$	$14^{(+)}$	9976.2
489.9	16.5(7)	0.57(5)	$M1$	$9^{(-)}$	$8^{(-)}$	7329.4
522.7	1.9(2)	0.89(20)	$(E1)$	$10^{(-)}$	10^+	7640.7
528.4	7.3(4)	0.57(4)	$M1$	$12^{(-)}$	$11^{(-)}$	8436.0
560.9	≈ 1			$13^{(+)}$		8934.2
561.3	6.1(4) [g]	0.62(30) [h]	$M1$	$12^{(+)}$	$11^{(+)}$	8334.7
581.8	1.2(2)	0.54(46)	$M1$	7^+	6^+	5102.3
592.4	16.2(6)	0.50(5)	$M1$	$14^{(+)}$	$13^{(+)}$	9526.6
599.5	10.2(5)	0.45(9)	$M1$	$13^{(+)}$	$12^{(+)}$	8934.2
605.1	13.4(6)	0.71(14)	$M1$	$8^{(-)}$	$7^{(-)}$	6839.5
616.7	4.1(3)	0.44(13)	$M1$	$17^{(+)}$	$16^{(+)}$	11354.4
655.4	9.1(5)	0.43(6)	$M1$	$11^{(+)}$	10^+	7773.4
659.8	4.7(3)	0.76(19)	$M1$	$13^{(+)}$	$13^{(+)}$	8934.2
761.5	7.7(5)	0.42(8)	$M1$	$16^{(+)}$	$15^{(+)}$	10737.7
782.9 [e]	5.8(4)	1.21(36)	$E2$	7^-	5^-	4367.0
841.2	4.7(3)	0.53(26)	$M1$	$13^{(+)}$	$12^{(+)}$	8934.2
850.4	78(2)	1.05(5)	$E2$	5^-	3^-	3584.1
897.7	100(2)	0.76(3)	$E1$	3^-	2^+	2733.7
936.4 [e]	8.3(6)	0.73(15)	$E1$	6^+	5^-	4520.5
		0.47(4) [i]				

TABLE I. (*Continued*).

E_γ [a] (keV)	I_γ [b]	R_{DCO} [c]	$\sigma\lambda$ [d]	J_i^π	J_f^π	E_i (keV)
972.9	1.9(2)	0.63(10)	$M1$ or $E1$	13	$12^{(-)}$	9408.9
1083.6 [e]	7.3(5)	0.32(10)	$E1$	7^+	6^-	5102.3
1132.1 [e]	4.2(4)		$(E1)$	$7^{(-)}$	7^+	6234.4
1255.5	1.7(2)				10^+	8373.5
1287.0	36(1)	0.68(5)	$E1$	8^+	7^-	5654.0
1464.0	17.8(9)	1.16(16)	$E2$	10^+	8^+	7118.0
1470.1 [e]	3.1(7)		$M1$ or $E1$	$8^{(-)}$		6839.5
1713.9 [e]	4.8(8)	0.71(7) [i] 1.06(8) [j]	$(E1)$	$7^{(-)}$	6^+	6234.4
1778.9	13.9(9)	1.10(22)	$E2$	10^+	8^+	7432.9
1836.0	142(5)		$E2$ [k]	2^+	0^+	1836.0
1867.4 [e]	4.5(4)		$(M1)$	$7^{(-)}$	7^-	6234.4
1902.9	2.2(3)		$M1$ or $E1$	$9^{(-)}$	8	7329.4
2153.4	4.0(6)	0.48(9) [i]	$M1$ or $E1$	$8^{(-)}$	7	6839.5
2473.3	1.5(3)		$(M1)$	$8^{(-)}$	7^-	6839.5
2733.7	$\leqslant 1$		$E3$	3^-	0^+	2733.7

[a] γ-ray energy. The error is between 0.1 and 0.5 keV.
[b] Relative intensity derived from a spectrum gated by the 1836.0 keV transition and normalized to the 897.7 keV transition.
[c] DCO ratio determined by gating on the 1836.0 keV transition except for the cases *i* and *j*.
[d] Multipolarity compatible with the DCO ratio and the deexcitation mode.
[e] Contaminated transition.
[f] Unresolved doublet. The intensity is estimated from coincidence spectra.
[g] Unresolved doublet. A combined value derived for the doublet is given.
[h] Combined value derived for the doublet.
[i] DCO ratio determined by gating on the 850.4 keV transition.
[j] DCO ratio determined by gating on the 936.4 keV transition.
[k] Taken from Ref. [9].

respective target-detector axis and the beam axis. The intensity $Y(\theta_2,\theta_1,\Phi)$ is obtained by exchanging the observation angles or the gating and observed transition.

The six Ge detectors of the OSIRIS CUBE are placed at angles of 45°, 90° and 135° relative to the beam direction, two at each angle. Taking into account the symmetry relation $Y(\theta_1,\theta_2,\Phi)=Y(180°-\theta_1,180°-\theta_2,\Phi)$ [26] there are eight detector pairs corresponding to $\theta_1=45°$, $\theta_2=90°$, $\Phi=90°$. Consequently, the γ-γ coincidence events were sorted into eight separate E_γ-E_γ matrices that are related to each of these detector pairs. To reduce the influence of the energy dependence of the time signals on the γ-γ coincidence efficiency of the different detector pairs, a relatively wide coincidence time interval of 400 ns was used. Coincidence spectra were extracted by setting gates on certain peak and background positions in the (45°,90°) matrices and the transposed (90°,45°) ones. These spectra were corrected for the energy-dependent efficiencies of the two detectors involved. To utilize the full statistics, all eight spectra related to a certain peak or background gate at one angle combination were added up. The DCO ratios were then obtained as the ratio of peak intensities in both background-corrected sum spectra. The coincidence spectra and the peak intensities were extracted using the code VS [22].

A DCO ratio of 1.0 is expected if both transitions γ_1 and γ_2 are stretched transitions of pure and equal multipole order. For the present detector geometry and completely aligned nuclei, a value of 0.6 is expected for a pure dipole transition gated on a stretched quadrupole transition. A value of 1.0 or 1.7 is expected for a $\Delta J=0$ transition using a gate on a $\Delta J=2$ or $\Delta J=1$ transition, respectively. The resulting DCO ratios for ^{88}Sr are given in Table I.

B. Lifetimes

Mean lifetimes were determined from Doppler shifts of γ rays observed in coincidence spectra at angles of 45° and 135° with respect to the beam direction using the DSA method. The coincidence spectra were extracted from two E_γ-E_γ matrices containing coincidence events of all Ge detector pairs that include one detector at 45° or 135°, respectively. Gates were set on the transitions at 1836.0, 897.7, 850.4, 434.6, 348.3, and 1287.0 keV. The corresponding coincidence spectra were added up to obtain maximum statistics. The lifetimes were deduced from comparing experimental line shapes with calculated ones in a joint fit at the two complementary observation angles of 45° and 135° (see Fig. 2). The velocity distributions of the emitting nuclei were calculated with a Monte Carlo code taking into account re-

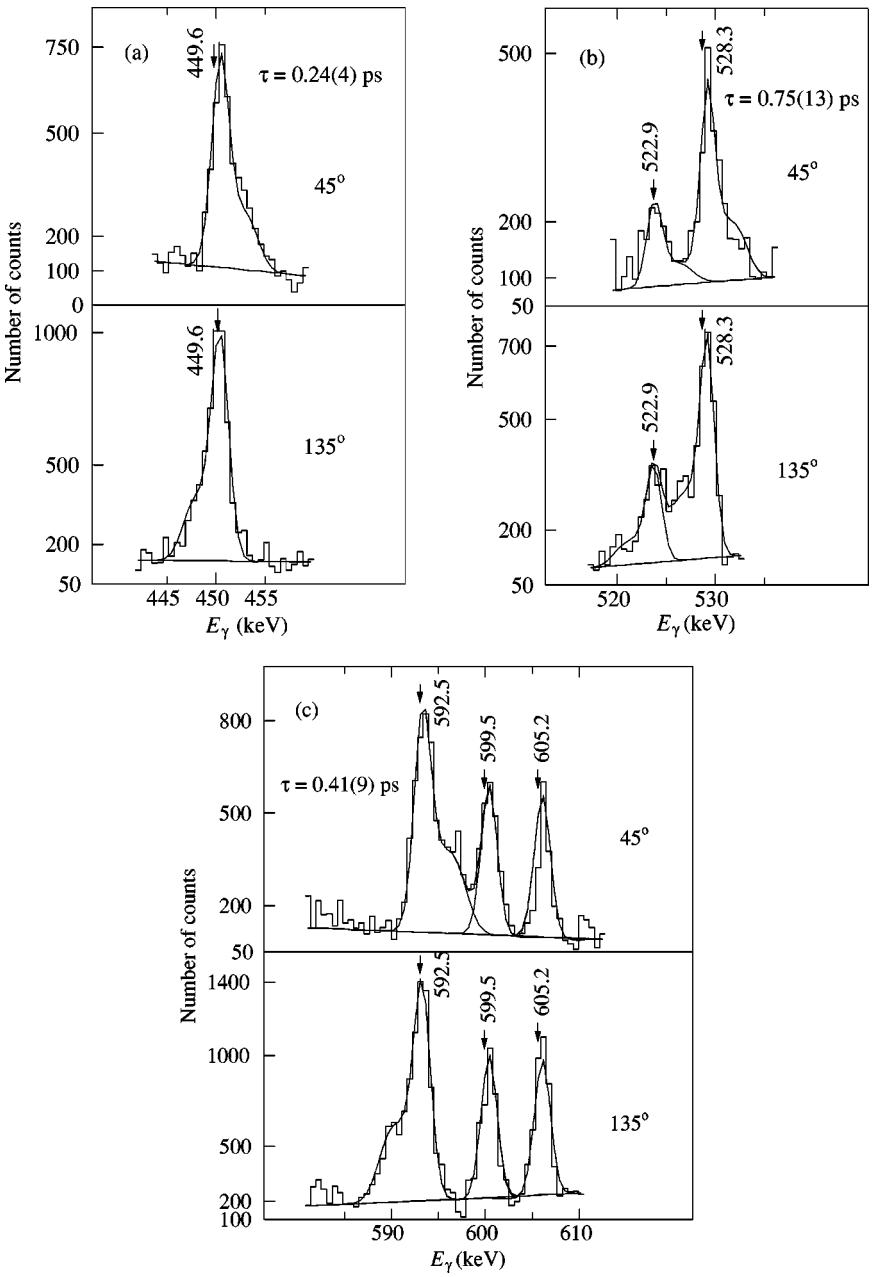

FIG. 2. Examples of the line-shape analysis using the DSA method. Lifetimes were deduced from a joint fit of calculated to experimental line shapes at the complementary observation angles of 45° and 135°. Feeding corrections are included. The given values of energies, lifetimes, and their errors result from the presented fits. The lifetimes refer to the adjacent peaks.

actions at different depths in the target, the kinematics of the reaction and the slowing down and deflection of the recoils [27]. For the slowing down process, Lindhard's cross sections [28] were used with correction factors of $f_e=0.9$ and $f_n=0.7$ for the electronic and nuclear stopping powers, respectively [1]. The sidefeeding times were neglected for excitation energies above 25 MeV. The latter value represents roughly the maximum excitation energy of the final nucleus $E^*=E^{\mathrm{CM}}_{^{11}\mathrm{B}}+Q-E_p-2E_n$ with $Q=-4.6$ MeV and mean energies of the emitted proton and neutrons of $E_p \approx 5$ MeV and $E_n \approx 2.5$ MeV, respectively. The sidefeeding time was assumed to increase with decreasing excitation energy according to $\tau_{sf}=(25-E/\mathrm{MeV})\times 0.03$ ps [1]. The lifetimes obtained from this analysis are given in Table II. Feeding corrections could be made for the lifetimes of the levels at 8436, 9527, and 9976 keV, while only effective lifetimes are given for the 8093, 8335, and 10738 keV levels.

C. The level scheme of ^{88}Sr

The extended level scheme of ^{88}Sr deduced from the present experiment is shown in Fig. 3. It results from γ-γ coincidence relations and γ-ray intensities. To assign spins and parities to the levels, γ-γ directional correlations and deexcitation modes were used.

The yrast sequence has been known up to the 5654 keV state from previous work with spin and parity assignments of $J^\pi=2^+$, 3^-, and 5^- for the 1836, 2734, and 3584 keV states, respectively [9]. In Ref. [13], tentative spin assignments of $J^\pi=(6)^-$ and $J^\pi=(7)^-$ were proposed for the levels at 4019 and 4367 keV, respectively. In a $(d,^6\mathrm{Li})$ study [29], a transferred angular momentum of $L=(7)$ was given for the 4367 keV level. For the 4019 keV level, however, the assignment $J^\pi=(5)^-$ was suggested in Ref. [29] as well as in an (n,γ) experiment [17] and was adopted in Ref. [9].

TABLE II. Lifetimes of states in ^{88}Sr.

E_{level} (keV)	E_γ (keV)	τ_{eff} [a] (ps)	τ [b] (ps)
8093	319.6	6.1(12) [d]	
8335	561.3 [c]	2.9(6)	
8436	528.4	2.0(7)	0.8(3) [e]
9527	592.4	2.06(16)	0.41(15)
9976	449.6	2.19(16)	0.25^{+15}_{-5}
10738	761.5	4.5(15)	

[a]Effective lifetime. The error in parentheses is the statistical error.
[b]Mean lifetime. The error in parentheses includes the statistical error, uncertainties of feeding times, feeding intensities, and a 10% uncertainty of the nuclear and electronic stopping power.
[c]This transition is part of a doublet with a 560.9 keV transition. It contains about 85% of the intensity of the doublet.
[d]This lifetime was deduced from a coincidence spectrum including the coincidence spectra gated on the peaks at 434.6 and 1836.0 keV.
[e]The lifetime of the feeding level at 9409 keV is assumed to be in the range of $\tau=(2-5)$ ps.

Based on the DCO ratios deduced for the 850.4, 434.6, and 348.3 keV transitions (see Table I) and the observation of a 782.9 keV crossover quadrupole transition in the present study, we assign $J^\pi=5^-$, 6^-, and 7^- to the 3584, 4019, and 4367 keV levels, respectively, in agreement with Ref. [13]. The DCO ratio of the 1287.0 keV transition indicates dipole character. Thus, $J=8$ is assigned to the 5654 keV level. This is compatible with the assignment of $J^\pi=8^+$ made for a 5652 keV level in an (e,e') experiment [30,31].

A sequence of six states on top of the 5654 keV yrast state was recently observed in Ref. [18] without spin assignments. The present measurement confirms the five levels at 7118, 7433, 7773, 8093, and 8274 keV. Based on the quadrupole character of the 1464.0 and 1778.9 keV transitions and the dipole character of the 655.4, 340.5, 319.6, and 181.4 keV transitions (see Table I) we propose the assignments of $J^\pi=10^+$, 10^+, $11^{(+)}$, $12^{(+)}$, and $13^{(+)}$ for the 7118, 7433, 7773, 8093, and 8274 keV levels, respectively. We do not confirm the placement of the 241.6 keV γ ray on top of the 181.4 keV transition and the placement of the 659.8 keV γ ray as a crossover transition linking the 7433 and 8093 keV levels as proposed in Ref. [18]. Instead, we found that the 241.6 and 659.8 keV γ rays deexcite levels at 8335 and 8934 keV, respectively. These levels form a new sequence together with levels at 9527, 9976, 10738, and 11354 keV as deduced from the present γ-γ coincidence data. The spin assignments for these levels are based on the dipole character of the 561.3, 841.2, 599.5, 592.4, 449.6, 761.5, and 616.7 keV transitions and are consistent with the DCO ratios of the 241.6 and 659.8 keV $\Delta J=0$ transitions (cf. Table I). The effective lifetime of 2.9 ps (cf. Table II) obtained for the 8335 keV state would result in lower limits of 0.42 W.u. or 0.0065 W.u. for the $B(M1)$ or $B(E1)$ values, respectively, of the 241.6 keV transition. The $B(E1)$ value of 6.5×10^{-3} W.u. is relatively high compared with values compiled for this mass region [32] while a $B(M1)$ value of 0.42 W.u. is also high but not unusual. Thus, positive parity seems more likely for the newly observed level sequence on top of the 8335 keV state and is tentatively proposed, although negative parity cannot be ruled out.

The level sequences feeding the 5^-, 6^-, and 7^- yrast states have been known from the recent fission experiment [18] and are confirmed on the basis of the present γ-γ coincidence relations. In addition to Ref. [18], a 581.8 keV transition connecting the 4521 and 5102 keV states as well as a 972.9 keV transition populating the 8436 keV state are observed. Spin assignments of $J=6$ and 7 for the 4521 and 5102 keV levels, respectively, are based on the DCO ratios of the 936.4, 581.8, and 1083.6 keV transitions. We propose positive parity to these levels since they are very likely to correspond to the $J^\pi=(6)^+$ state at 4514(5)/4518(2) keV and $J^\pi=(7)^+$ state at 5094(6)/5100(3) keV, respectively, observed in (d,p) experiments [15,16]. A $J^\pi=7^+$ state at 5109 keV was also found in an (e,e') experiment [30]. The dipole character of the 1713.9 keV transition suggests $J=7$ for the level at 6234 keV. The DCO values of the 605.1, 489.9, 311.3, 266.9, and 528.4 keV transitions indicate dipole character as well, resulting in assignments of $J=8$, 9, 10, 11, and 12 for the states at 6840, 7329, 7641, 7908, and 8436 keV, respectively. In several neighboring nuclei as in the isotones ^{86}Kr [5], ^{89}Y [8], and ^{90}Zr [33], negative-parity sequences have been found in competition with the positive-parity excitations. Since positive parity has been assigned to states up to the 17^+ state at 11354 keV (except for the 3^- to 7^- states), we consider the levels with $J=7$ to 12 on top of the 6234 keV level as candidates for a negative-parity level sequence.

Based on the DCO values of the 2153.4 and 324.2 keV transitions, we assign $J=7$ and 8 for the 4687 and 5427 keV levels, respectively.

III. DISCUSSION

A. Shell-model calculations for ^{88}Sr

Shell-model studies were previously carried out to interpret excited states in ^{88}Sr up to 6 MeV [34–37]. The calculations in Ref. [34] were made without any interaction between the proton and the neutron systems. Proton configurations only were considered in Refs. [36,37]. Shell-model calculations for states up to 5 MeV in the model space $(0f_{5/2},1p_{3/2},1p_{1/2},0g_{9/2})$ for the protons and $(1p_{1/2},0g_{9/2},1d_{5/2},1s_{1/2},1d_{3/2},0g_{7/2})$ for the neutrons were performed in Ref. [13] without considering 2p-2h excitations. Quasiparticle-phonon model calculations performed in Ref. [18] include 20 orbitals up to $0j_{15/2}$ for both the proton and neutron system [38] to construct one-, two-, and three-phonon excitations for the states up to 8.5 MeV.

The shell-model space used in our calculations includes the active proton orbitals $\pi(0f_{5/2},1p_{3/2},1p_{1/2},0g_{9/2})$ and neutron orbitals $\nu(1p_{1/2},0g_{9/2},1d_{5/2})$ relative to a hypothetic ^{66}Ni core. Since an empirical set of effective interaction matrix elements for this model space is not available up to now various empirical sets have been combined with the matrix elements of a modified surface-delta interaction. Details of this procedure are described in Refs. [5,6]. The effective interaction in the proton shells was taken from Ref.

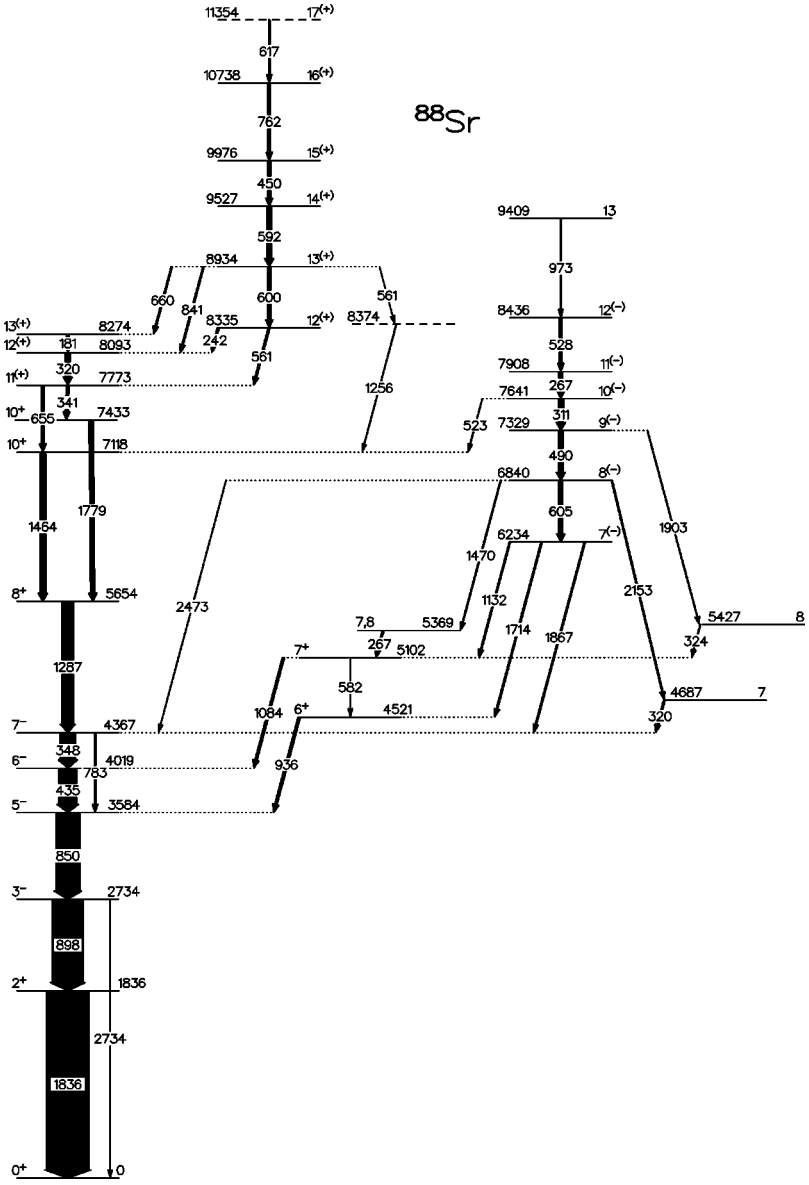

FIG. 3. Level scheme of ^{88}Sr deduced from the present experiment.

[36]. In that work, the residual interaction and the single-particle energies of the proton orbitals were deduced from a least-squares fit to 170 experimental level energies in $N=50$ nuclei with mass numbers between 82 and 96. The data given in Ref. [39] have been used for the proton-neutron interaction between the $\pi(1p_{1/2},0g_{9/2})$ and the $\nu(1p_{1/2},0g_{9/2})$ orbitals. These data were derived from an iterative fit to 95 experimental level energies of $N=48$, 49, and 50 nuclei. The matrix elements of the neutron-neutron interaction of the $\nu(1p_{1/2},0g_{9/2})$ orbitals have been assumed to be equal to the isospin $T=1$ component of the proton-neutron interaction given in Ref. [39]. For the $(\pi 0f_{5/2},\nu 0g_{9/2})$ residual interaction, the matrix elements proposed in Ref. [40] have been used.

The single-particle energies relative to the ^{66}Ni core have been derived from the single-particle energies of the proton orbitals given in Ref. [36] with respect to the ^{78}Ni core and from the neutron single-hole energies of the $1p_{1/2},0g_{9/2}$ orbitals [39]. The transformation of these single-particle energies to those relative to the ^{66}Ni core has been performed [41] on the basis of the effective residual interactions given above. The obtained values are $\epsilon^{\pi}_{0f_{5/2}}=-9.106$ MeV, $\epsilon^{\pi}_{1p_{3/2}}=-9.033$ MeV, $\epsilon^{\pi}_{1p_{1/2}}=-4.715$ MeV, $\epsilon^{\pi}_{0g_{9/2}}=-0.346$ MeV, $\epsilon^{\nu}_{1p_{1/2}}=-7.834$ MeV, $\epsilon^{\nu}_{0g_{9/2}}=-6.749$ MeV, and $\epsilon^{\nu}_{1d_{5/2}}=-4.144$ MeV. These single-particle energies and the corresponding values of the strengths of the residual interactions have been used to calculate level energies as well as $M1$ and $E2$ transition strengths. For the latter, effective g factors of $g_s^{\rm eff}=0.7g_s^{\rm free}$ and effective charges of $e_{\pi}=1.72e$ and $e_{\nu}=1.44e$ [42], have been applied.

The nucleus ^{88}Sr has 10 protons and 12 neutrons in the considered configuration space. To make the calculations feasible, a truncation of the occupation numbers was necessary. At most three protons are allowed to occupy the $(1p_{1/2},0g_{9/2})$ subshell and at most one $0g_{9/2}$ neutron can be lifted to the $1d_{5/2}$ orbital. With these restrictions, a configu-

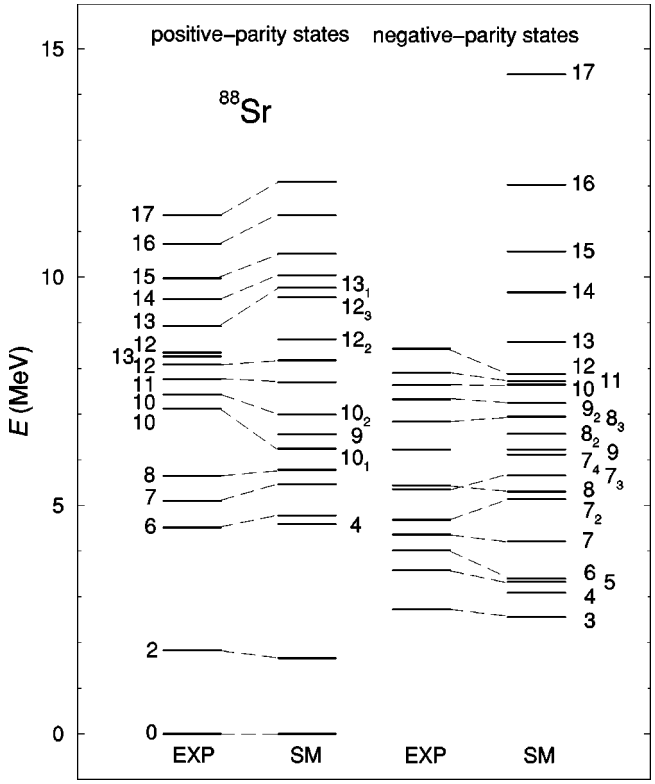

FIG. 4. Comparison of experimental with calculated level energies in ^{88}Sr.

ration space with dimensions smaller than 7000 has been obtained. The calculations were carried out with the code RITSSCHIL [43].

B. Results

Experimental and calculated level energies of states in ^{88}Sr are compared in Fig. 4. The main components of the shell-model positive-parity and negative-parity states are listed in Tables III and IV, respectively. Calculated transition strengths are compared with experimental ones in Table V.

The calculated 2_1^+ yrast state is mainly described by the $\pi(1p_{3/2}^{-1}1p_{1/2}^1)$ excitation. Small contributions including the neutron-core excitation $(0g_{9/2}^{-1}1d_{5/2}^1)$ add up to some 8%. This is about half of the 17% occupation obtained from the spectroscopic factor derived in a (d,p) experiment [16]. The calculated $B(E2,2_1^+\rightarrow 0_1^+)$ strength is in good agreement with the experimental value given in Ref. [9] (see Table V). To create a 4_1^+ state the break up of an additional proton pair is necessary. Thus the configuration $\pi(0f_{5/2}^{-1}1p_{3/2}^{-1}0g_{9/2}^2)$ dominates the 4_1^+ state which, however, has not been observed in the present experiment. The lowest-lying 6^+ and 7^+ states are predicted to contain the neutron-core excitation $\nu(0g_{9/2}^{-1}1d_{5/2}^1)$ as the main component although the proton excitation dominating the 4^+ yrast state could generate 6^+ and 7^+ states as well. The calculated contribution of the $\nu(0g_{9/2}^{-1}1d_{5/2}^1)$ configuration to the 6^+ and 7^+ states is consistent with spectroscopic factors extracted in the (d,p) experiment [16]. These highest-spin members of the $\nu(0g_{9/2}^{-1}1d_{5/2}^1)$ multiplet become yrast in ^{88}Sr as well as in the lighter $N=50$ neighbor ^{86}Kr [5], while the heavier $N=50$ neighbor ^{90}Zr shows a different behavior [33].

The lowest-lying 8^+, 9^+, 10^+, and 12^+ states as well as the second 12^+ state are characterized by the proton configuration $\pi(0f_{5/2}^{-2}0g_{9/2}^2)$ while the second 10^+ state and the first 11^+ state contain mainly the proton configuration $\pi(0f_{5/2}^{-1}1p_{3/2}^{-1}0g_{9/2}^2)$. The 10_1^+ and 10_2^+ states are predicted considerably below the experimental states whereas the calculated 8_1^+, 11_1^+, and 12_1^+ states reproduce well the experimental ones. The calculated values of $B(M1,12_2^+\rightarrow 12_1^+)=0.12$ W.u. and $B(M1,12_2^+\rightarrow 11_1^+)=0.02$ W.u. are not far from the experimental lower limits of $B(M1)=0.42$ W.u. and $B(M1)=0.03$ W.u. for the 241.6 and 561.3 keV transitions, respectively. In addition, the calculated second 12_2^+ state fits well the energy of the experimental 8335 keV state (cf. Fig. 4). Since the proton configurations discussed above are exhausted at $J^\pi=12^+$, the generation of positive-parity states with higher spin requires the break up of an additional pair of nucleons. In fact, proton configurations as well as neutron-core excitations form the major contribution to the positive-parity states with $J\geqslant 13$. The lowest-lying 13^+, 14^+, 15^+, and 16^+ states as well as the 12_3^+ state contain the configuration $\pi(0f_{5/2}^{-2}0g_{9/2}^2)\nu(0g_{9/2}^{-1}1d_{5/2}^1)$ as the main component while the configuration $\pi(0f_{5/2}^{-1}1p_{3/2}^{-1}0g_{9/2}^2)\nu(0g_{9/2}^{-1}1d_{5/2}^1)$ dominates the 13_2^+ and the lowest 17^+ state. The calculated 13^+, 14^+, 15^+, 16^+, and 17^+ states may correspond to the experimental sequence of states at 8934, 9527, 9976, 10738, and 11354 keV. In this case, we cannot assign any calculated state to the experimental 13^+ state at 8274 keV which is about 1.5 MeV below the calculated 13_1^+ state. As discussed above, the calculated 12_2^+ state may correspond to the experimental 8335 keV level which in this case would have a structure different from that of the level sequence on top of it. As a consequence, the calculated transition strength of $B(M1)\approx 2\times 10^{-5}$ W.u. for the $13_1^+\rightarrow 12_2^+$ transition would correspond to a lifetime of $\tau\approx 200$ ps for the 8934 keV state. This is, however, in discrepancy to the effective lifetime of 2.9(6) ps deduced for the 8335 keV level (see Table II). The calculations predict the 12_3^+ state to have the same structure as that of the 13_1^+, 14_1^+, 15_1^+, 16_1^+, and 17_1^+ states. An assignment of the calculated 12_3^+ state to the experimental 8335 keV state would lead to a disagreement between the experimental value of $B(M1)>0.42$ W.u. and the calculated one of $B(M1)\approx 9\times 10^{-3}$ W.u. for the 241.6 keV transition. Thus, we cannot make a clear conclusion on the structure of the 8335 keV state. The calculated $B(M1)$ values for the $15_1^+\rightarrow 14_1^+$ and $14_1^+\rightarrow 13_1^+$ transitions are in reasonable agreement with the experimental transition strengths (see Table V), although they decrease with increasing spin in contrast to the experiment. The predicted transition strength of 0.02 W.u. for the $14_1^+\rightarrow 13_2^+$ transition is not compatible with the experimental value of 0.37(14) W.u. of the 592.4 keV transition. This may suggest that the calculated 13_1^+ state corresponds to the 8934 keV level. The experimental $B(M1)$ value of the 592.4 keV transition would also be fairly well reproduced by the calculated value of $B(M1,14_1^-\rightarrow 13_2^-)=0.18$ W.u., if negative

TABLE III. Main components of wave functions of positive-parity states in ^{88}Sr.

J^π	Configuration [a]		υ [b]	A [c]
2_1^+	$\pi[1p_{3/2}^{-1}1p_{1/2}^{1}]$		2	73
4_1^+	$\pi[(0f_{5/2}^{-1}1p_{3/2}^{-1})_4(0g_{9/2}^{2})_0]$		2	23
6_1^+	$\nu[0g_{9/2}^{-1}1d_{5/2}^{1}]$		2	58
7_1^+	$\nu[0g_{9/2}^{-1}1d_{5/2}^{1}]$		2	55
8_1^+	$\pi[(0f_{5/2}^{-2})_2(0g_{9/2}^{2})_6]$		4	18
9_1^+	$\pi[(0f_{5/2}^{-2})_4(0g_{9/2}^{2})_6]$		4	20
10_1^+	$\pi[(0f_{5/2}^{-2})_2(0g_{9/2}^{2})_8]$		4	47
10_2^+	$\pi[(0f_{5/2}^{-1}1p_{3/2}^{-1})_4(0g_{9/2}^{2})_8]$		4	31
11_1^+	$\pi[(0f_{5/2}^{-1}1p_{3/2}^{-1})_4(0g_{9/2}^{2})_8]$		4	38
12_1^+	$\pi[(0f_{5/2}^{-2})_4(0g_{9/2}^{2})_8]$		4	40
12_2^+	$\pi[(0f_{5/2}^{-2})_4(0g_{9/2}^{2})_8]$		4	28
12_3^+	$\pi[(0f_{5/2}^{-2})_0(0g_{9/2}^{2})_8]$	$\nu[0g_{9/2}^{-1}1d_{5/2}^{1}]_5$	4	7
	$\pi[(0f_{5/2}^{-2})_2(0g_{9/2}^{2})_8]$	$\nu[0g_{9/2}^{-1}1d_{5/2}^{1}]_5$	6	7
13_1^+	$\pi[(0f_{5/2}^{-2})_2(0g_{9/2}^{2})_8]$	$\nu[0g_{9/2}^{-1}1d_{5/2}^{1}]_5$	6	16
13_2^+	$\pi[(0f_{5/2}^{-1}1p_{3/2}^{-1})_1(0g_{9/2}^{2})_6]$	$\nu[0g_{9/2}^{-1}1d_{5/2}^{1}]_6$	6	7
14_1^+	$\pi[(0f_{5/2}^{-2})_2(0g_{9/2}^{2})_8]$	$\nu[0g_{9/2}^{-1}1d_{5/2}^{1}]_6$	6	19
15_1^+	$\pi[(0f_{5/2}^{-2})_2(0g_{9/2}^{2})_8]$	$\nu[0g_{9/2}^{-1}1d_{5/2}^{1}]_6$	6	29
16_1^+	$\pi[(0f_{5/2}^{-2})_2(0g_{9/2}^{2})_8]$	$\nu[0g_{9/2}^{-1}1d_{5/2}^{1}]_6$	6	20
17_1^+	$\pi[(0f_{5/2}^{-1}1p_{3/2}^{-1})_4(0g_{9/2}^{2})_8]$	$\nu[0g_{9/2}^{-1}1d_{5/2}^{1}]_6$	6	15

[a]Main contribution to the wave function.
[b]Seniority.
[c]Amount of the contribution in percent.

parity were assumed for the discussed level sequence. However, in this case the calculated value of $B(M1,15_1^- \rightarrow 14_1^-) = 0.04$ W.u. and the experimental one of $1.4^{+0.3}_{-0.8}$ W.u. for the 449.6 keV transition would be in obvious disagreement.

The lowest observed negative-parity state in ^{88}Sr is the 3^- state. For this state, the proton excitation $(1p_{3/2}^{-1}0g_{9/2}^{1})$ is predicted as the main component which is consistent with the findings in transfer reactions [44,45]. In Ref. [30], a transition strength of $B(E3) = 22.61(12)$ W.u. was measured for the transition depopulating the 3^- state to the ground state indicating a collective octupole vibrational structure. In contrast to previous shell model studies [34–37], the present calculations predict the 3^- state slightly below the experimental one as is also obtained in QPM calculations [18]. The lowest-lying 5^- state is characterized by the $\pi(1p_{3/2}^{-1}0g_{9/2}^{1})$ configuration in the present calculations, as previously found in the ^{87}Rb(^{3}He,d) experiment [44]. The main configuration in the calculated 6^- and 7^- states is $\pi(0f_{5/2}^{-1}0g_{9/2}^{1})$. The energies of the experimental 5^- and 7^- states are reasonably well reproduced while the 6^- state is calculated about 1 MeV below the experimental one.

To create negative-parity states of spin higher than $J=7$, the breakup of an additional pair of nucleons is necessary. The 7_2^-, 8_1^-, 8_2^-, and 9_1^- states are dominated by the $\pi(0f_{5/2}^{-1}1p_{3/2}^{-1}1p_{1/2}^{1}0g_{9/2}^{1})$ configuration while the main component of the 7_3^- state is the $\pi(1p_{3/2}^{-2}1p_{1/2}^{1}0g_{9/2}^{1})$ configuration. The calculated 7_2^-, 7_3^-, and 8_1^- states might correspond to the experimental states at 4687, 5369, and 5427 keV, respectively.

The level sequence built on top of the 6234 keV state depopulates mainly through the 6^+ and 7^+ members of the neutron $(0g_{9/2}^{-1}1d_{5/2}^{1})$ multiplet to the 5^- and 6^- proton states. This suggests possible seniority $\upsilon=4$ contributions to the structure of these states arising from neutron-core excitations coupled to proton excitations. The calculations predict this seniority $\upsilon=4$ structure of negative parity for the discussed level sequence except for the 7^- state. In fact, the calculations yield no neutron contributions to the structure of the first six 7^- states. The 6234 keV state may correspond to the calculated 7_4^- or 7_5^- states, dominated by the $\pi(1p_{3/2}^{-2}1p_{1/2}^{1}0g_{9/2}^{1})$ and $\pi(0f_{5/2}^{-2}1p_{1/2}^{1}0g_{9/2}^{1})$ configurations, respectively, or to a higher lying calculated 7^- state including proton as well as neutron configurations. The $\pi(1p_{3/2}^{-1}0g_{9/2}^{1})$ $\nu(0g_{9/2}^{-1}1d_{5/2}^{1})$ configuration predominates in the calculated 8_3^- and 9_2^- states while the main component of the 10_1^-, 11_1^-, and 13_1^- states is $\pi(0f_{5/2}^{-1}0g_{9/2}^{1})$ $\nu(0g_{9/2}^{-1}1d_{5/2}^{1})$. The predicted 12_1^- and 12_2^- states include mainly excitations of the type $\pi(1p_{3/2}^{-1}0g_{9/2}^{1})_6$ $\nu(0g_{9/2}^{-1}1d_{5/2}^{1})_6$. Thus, the calculated 8_3^-, 9_2^-, 10_1^-, 11_1^-, and 12_1^- states may correspond to the experimental 8^- to 12^- states. As can be seen in Fig. 4, these calculated states reproduce the energies of the experimental states fairly well. The large experimental transition strength of $B(M1) = 0.27(10)$ W.u. deduced for the 528.4 keV $12^{(-)} \rightarrow 11^{(-)}$ transition (see Table V) can only be reproduced by the proton-neutron $\upsilon=4$ configuration given above. In this way, the calculations are compatible with the assignment of negative parity tentatively proposed in Sec. II C for this sequence

TABLE IV. Main components of wave functions of negative-parity states in ^{88}Sr.

J^π	Configuration [a]		υ [b]	A [c]
3_1^-	$\pi[1p_{3/2}^{-1}0g_{9/2}^{1}]$		2	57
5_1^-	$\pi[1p_{3/2}^{-1}0g_{9/2}^{1}]$		2	52
6_1^-	$\pi[0f_{5/2}^{-1}0g_{9/2}^{1}]$		2	64
7_1^-	$\pi[0f_{5/2}^{-1}0g_{9/2}^{1}]$		2	63
7_2^-	$\pi[(0f_{5/2}^{-1}1p_{3/2}^{-1})_4(1p_{1/2}^{1}0g_{9/2}^{1})_5]$		4	21
7_3^-	$\pi[(1p_{3/2}^{-2})_2(1p_{1/2}^{1}0g_{9/2}^{1})_5]$		4	52
7_4^-	$\pi[(0f_{5/2}^{-1}1p_{3/2}^{-1})_4(1p_{1/2}^{1}0g_{9/2}^{1})_4]$		4	25
7_5^-	$\pi[(0f_{5/2}^{-2})_2(1p_{1/2}^{1}0g_{9/2}^{1})_5]$		4	19
8_1^-	$\pi[(0f_{5/2}^{-1}1p_{3/2}^{-1})_4(1p_{1/2}^{1}0g_{9/2}^{1})_5]$		4	62
8_2^-	$\pi[(0f_{5/2}^{-1}1p_{3/2}^{-1})_3(1p_{1/2}^{1}0g_{9/2}^{1})_5]$		4	47
8_3^-	$\pi[1p_{3/2}^{-1}0g_{9/2}^{1}]_3$	$\nu[0g_{9/2}^{-1}1d_{5/2}^{1}]_6$	4	32
9_1^-	$\pi[(0f_{5/2}^{-1}1p_{3/2}^{-1})_4(1p_{1/2}^{1}0g_{9/2}^{1})_5]$		4	65
9_2^-	$\pi[1p_{3/2}^{-1}0g_{9/2}^{1}]_3$	$\nu[0g_{9/2}^{-1}1d_{5/2}^{1}]_6$	4	16
10_1^-	$\pi[0f_{5/2}^{-1}0g_{9/2}^{1}]_6$	$\nu[0g_{9/2}^{-1}1d_{5/2}^{1}]_5$	4	18
11_1^-	$\pi[0f_{5/2}^{-1}0g_{9/2}^{1}]_6$	$\nu[0g_{9/2}^{-1}1d_{5/2}^{1}]_5$	4	32
12_1^-	$\pi[1p_{3/2}^{-1}0g_{9/2}^{1}]_6$	$\nu[0g_{9/2}^{-1}1d_{5/2}^{1}]_6$	4	43
12_2^-	$\pi[1p_{3/2}^{-1}0g_{9/2}^{1}]_6$	$\nu[0g_{9/2}^{-1}1d_{5/2}^{1}]_6$	4	27
13_1^-	$\pi[0f_{5/2}^{-1}0g_{9/2}^{1}]_6$	$\nu[0g_{9/2}^{-1}1d_{5/2}^{1}]_7$	4	31
13_2^-	$\pi[(0f_{5/2}^{-1}1p_{3/2}^{-1})_4(1p_{1/2}^{1}0g_{9/2}^{1})_5]$	$\nu[0g_{9/2}^{-1}1d_{5/2}^{1}]_5$	6	23
14_1^-	$\pi[(0f_{5/2}^{-1}1p_{3/2}^{-1})_4(1p_{1/2}^{1}0g_{9/2}^{1})_5]$	$\nu[0g_{9/2}^{-1}1d_{5/2}^{1}]_6$	6	40
15_1^-	$\pi[(0f_{5/2}^{-1}1p_{3/2}^{-1})_4(1p_{1/2}^{1}0g_{9/2}^{1})_5]$	$\nu[0g_{9/2}^{-1}1d_{5/2}^{1}]_7$	6	39
16_1^-	$\pi[(0f_{5/2}^{-1}1p_{3/2}^{-1})_4(1p_{1/2}^{1}0g_{9/2}^{1})_5]$	$\nu[0g_{9/2}^{-1}1d_{5/2}^{1}]_7$	6	74
17_1^-	$\pi[0f_{5/2}^{-3}0g_{9/2}^{3}]_{11}$	$\nu[0g_{9/2}^{-1}1d_{5/2}^{1}]_6$	8	8

[a]Main contribution to the wave function.
[b]Seniority.
[c]Amount of the contribution in percent.

of states. Configurations of the type $\pi(0f_{5/2}^{-1}1p_{3/2}^{-1}1p_{1/2}^{1}0g_{9/2}^{1})$ $\nu(0g_{9/2}^{-1}1d_{5/2}^{1})$ are obtained for the calculated 13_2^-, 14_1^-, 15_1^-, and 16_1^- states, while the $\upsilon=8$ configuration $\pi(0f_{5/2}^{-3}0g_{9/2}^{3})$ $\nu(0g_{9/2}^{-1}1d_{5/2}^{1})$ is predicted for the main component of the 17_1^- state in our calculations.

IV. SUMMARY

High-spin states of ^{88}Sr have been studied via the reaction ^{80}Se(^{11}B,$p2n$) at a beam energy of 45 MeV. The level scheme of ^{88}Sr has been extended by a new level sequence built on top of the 8335 keV level up to $E\approx 11$ MeV and $J=17$. On the basis of a DCO analysis, the spins of all excited states above the 7^- level at 4367 keV were determined for the first time. Mean lifetimes of three levels have been derived using the Doppler-shift-attenuation method. These lifetimes result in large $M1$ transition strengths of $B(M1)\approx 0.3$ to 1.4 W.u. for the corresponding transitions.

Excited states in ^{88}Sr were interpreted in the framework of the shell model. The calculations were performed in a model space including the $(0f_{5/2},1p_{3/2},1p_{1/2},g_{9/2})$ orbitals for the protons and the $(1p_{1/2},0g_{9/2},1d_{5/2})$ orbitals for the neutrons. Neutron-core excitations are predicted for the lowest 6^+ and 7^+ states in agreement with results of previous (d,p) experiments [14–17]. Proton configurations of seniority $\upsilon=4$ are predicted for the positive-parity states with $J^\pi=8^+$, 10^+, 11^+, and 12^+. The experimental high-spin level sequences with $J^\pi>7^-$ and $J^\pi\geqslant 12^+$ linked by strong $M1$ transitions are described by the calculations as $\upsilon=4$ and 6 multiplets, respectively, which include proton excitations coupled to neutron-core excitations.

TABLE V. Experimental and calculated transition strengths in ^{88}Sr.

E_γ (keV)	J_i^π	J_f^π	$\sigma\lambda$	$B(\sigma\lambda)_{\rm EXP}$ [a] (W.u.)	$B(\sigma\lambda)_{\rm SM}$ [b] (W.u.)
1836.0	2_1^+	0_1^+	$E2$	7.20(22) [c]	10.3
897.7	3_1^-	2_1^+	$E1$	0.0006(3) [c]	
2733.7	3_1^-	0_1^+	$E3$	22.61(12) [c]	
850.4	5_1^-	3_1^-	$E2$	0.39(11) [c]	1.45
528.4	$12_1^{(-)}$	$11_1^{(-)}$	$M1$	0.27(10) [d]	0.35
592.4	$14_1^{(+)}$	$13_1^{(+)}$	$M1$	0.37(14) [d]	1.02
449.6	$15_1^{(+)}$	$14_1^{(+)}$	$M1$	$1.4^{+0.3}_{-0.8}$ [d]	0.66

[a]Experimental transition strengths in Weisskopf units (W.u.). 1 W.u.$(M1)=1.79\ \mu_N^2$; 1 W.u.$(E1)=1.27\ e^2$fm^2; 1 W.u.$(E2)=22.90\ e^2$fm^4.
[b]Calculated transition strengths in Weisskopf units. Values of $g_s^{\rm eff}=0.7g_s^{\rm free}$ and $e_\pi=1.72e, e_\nu=1.44e$ have been used for the $B(M1)$ and $B(E2)$ values, respectively.
[c]Value taken from Ref. [9].
[d]Value obtained from the present experiment.

ACKNOWLEDGMENTS

The authors would like to thank W. Schulze, M. Freitag, and G. Pascovici for the technical assistance. E.A.S. acknowledges financial support by the Sächsisches Staatsministerium für Wissenschaft und Kunst under Contract No. 4-7531.50-04-844-99/16 and by the Forschungszentrum Rossendorf. W.A. acknowledges financial support by the Bulgarian NRF under Contract No. PH 908 and by the FZ Rossendorf.

[1] G. Winter, J. Döring, F. Dönau, and L. Funke, Z. Phys. A **334**, 415 (1989).
[2] R. Schwengner, G. Winter, J. Reif, H. Prade, L. Käubler, R. Wirowski, N. Nicolay, S. Albers, S. Eßer, P. von Brentano, and W. Andrejtscheff, Nucl. Phys. **A584**, 159 (1995).
[3] R. Schwengner, G. Winter, J. Reif, H. Prade, L. Käubler, R. Wirowski, N. Nicolay, S. Albers, S. Eßer, P. von Brentano, and W. Andrejtscheff, Phys. Scr. **T56**, 126 (1995).
[4] R. Schwengner, J. Reif, H. Schnare, G. Winter, T. Servene, L. Käubler, H. Prade, M. Wilhelm, A. Fitzler, S. Kasemann, E. Radermacher, and P. von Brentano, Phys. Rev. C **57**, 2892 (1998).
[5] G. Winter, R. Schwengner, J. Reif, H. Prade, L. Funke, R. Wirowski, N. Nicolay, A. Dewald, P. von Brentano, H. Grawe, and R. Schubart, Phys. Rev. C **48**, 1010 (1993).
[6] G. Winter, R. Schwengner, J. Reif, H. Prade, J. Döring, R. Wirowski, N. Nicolay, P. von Brentano, H. Grawe, and R. Schubart, Phys. Rev. C **49**, 2427 (1994).
[7] L. Funke, G. Winter, J. Döring, L. Käubler, H. Prade, R. Schwengner, E. Will, Ch. Protochristov, W. Andrejtscheff, L.G. Kostova, P.O. Lipas, and R. Wirowski, Nucl. Phys. **A541**, 241 (1992).
[8] J. Reif, G. Winter, R. Schwengner, H. Prade, and L. Käubler, Nucl. Phys. **A87**, 449 (1995).
[9] H.W. Müller and J.W. Tepel, Nucl. Data Sheets **54**, 1 (1988).
[10] S.P. Fivozinsky, S. Penner, J.W. Lightbody, Jr., and D. Blum, Phys. Rev. C **9**, 1533 (1974).
[11] F.R. Metzger, Phys. Rev. C **15**, 2253 (1977).
[12] H. Mach, F.K. Wohn, G. Molnár, K. Sistemich, J.C. Hill, M. Moszyński, R.L. Gill, W. Krips, and D.S. Brenner, Nucl. Phys. **A523**, 197 (1991).
[13] S.A. Arnell, A. Nilsson, and O. Stankiewicz, Nucl. Phys. **A241**, 109 (1975).
[14] E.R. Cosman and D.C. Slater, Phys. Rev. **172**, 1126 (1968).
[15] Kamal K. Seth, Kurt A. Buzard, J. Picard, and G. Bassani, Phys. Rev. C **10**, 1928 (1974).
[16] P.C. Li and W.W. Daehnick, Nucl. Phys. **A462**, 26 (1987).
[17] Ch. Winter, B. Krusche, K.P. Lieb, T. Weber, G. Hlawatsch, T. von Egidy, and F. Hoyler, Nucl. Phys. **A473**, 129 (1987).
[18] E.A. Stefanova, T. Kutsarova, I. Deloncle, M.-G. Porquet, M. Grinberg, A. Minkova, T. Venkova, B.J.P. Gall, A. Wilson, F. Hoellinger, N. Schulz, H. Sergolle, J. Duprat, F. Azaiez, S. Bouneau, C. Bourgeois, C. Gautherin, R. Lucas, and Ch. Stoyanov, Nucl. Phys. **A669**, 14 (2000).
[19] R. Wirowski, Ph.D. thesis, Universität zu Köln, 1993.
[20] M.W. Luig, S. Albers, F. Giesen, N. Nicolay, J. Rest, R. Wirowski, and P. von Brentano, Verh. Dtsch. Phys. Ges. **30**, 736 (1995).
[21] D.C. Radford, Nucl. Instrum. Methods Phys. Res. A **361**, 297 (1995).
[22] J. Theuerkauf, S. Esser, S. Krink, M. Luig, N. Nicolay, and H. Wolters, Program VS (version 6.65), Universität zu Köln, 1992.
[23] R.M. Steffen and K. Alder, in *The Electromagnetic Interaction in Nuclear Spectroscopy*, edited by W.D. Hamilton (North-Holland, Amsterdam, 1975), p. 505.
[24] K.S. Krane, R.M. Steffen, and R.M. Wheeler, Nucl. Data Tables **11**, 351 (1973).
[25] A. Krämer-Flecken, T. Morek, R.M. Lieder, W. Gast, G. Hebbinghaus, H.M. Jäger, and W. Urban, Nucl. Instrum. Methods Phys. Res. A **275**, 333 (1989).
[26] L.P. Ekström and A. Nordlund, Nucl. Instrum. Methods Phys. Res. A **313**, 421 (1992).
[27] G. Winter, Nucl. Instrum. Methods Phys. Res. A **214**, 537 (1983).
[28] J. Lindhard, V. Nielsen, and M. Scharff, Mat. Fys. Medd. K. Dan. Vidensk. Selsk. **36**, 1 (1968).
[29] A.M. van den Berg, A. Saha, G.D. Jones, L.W. Put, and R.H. Siemssen, Nucl. Phys. **A429**, 1 (1984).
[30] L.T. van der Bijl, Ph.D. thesis, Vrije Universiteit, Amsterdam, 1982.
[31] T.E. Milliman, J.H. Heisenberg, F.W. Hersman, J.P. Connelly, C.N. Papanicolas, J.E. Wise, H.P. Blok, and L.T. van der Bijl, Phys. Rev. C **32**, 805 (1985).
[32] P.M. Endt, At. Data Nucl. Data Tables **23**, 547 (1979).
[33] E.K. Warburton, J.W. Olness, C.J. Lister, R.W. Zurmühle, and J.A. Becker, Phys. Rev. C **31**, 1184 (1985).
[34] T.A. Huges, Phys. Rev. **181**, 1586 (1969).
[35] N. Auerbach and J.P. Vary, Phys. Rev. C **13**, 1709 (1976).
[36] Xiangados Ji and B.H. Wildenthal, Phys. Rev. C **37**, 1256 (1988).
[37] J. Sinatkas, L.D. Skouras, D. Strottman, and J.D. Vergados, J. Phys. G **18**, 1377 (1992).
[38] M. Grinberg (private communications).
[39] R. Gross and A. Frenkel, Nucl. Phys. **A267**, 85 (1976).
[40] P.C. Li, W.W. Daehnick, S.K. Saha, J.D. Brown, and R.T. Kouzes, Nucl. Phys. **A469**, 393 (1987).
[41] J. Blomqvist and L. Rydström, Phys. Scr. **31**, 31 (1985).
[42] D.H. Gloeckner and F.J.D. Serduke, Nucl. Phys. **A220**, 477 (1974).
[43] D. Zwarts, Comput. Phys. Commun. **38**, 365 (1985).
[44] M.J. Schneider, R.E. Anderson, and P.G. Brabeck, Nucl. Phys. **A246**, 156 (1975).
[45] W.P. Alford, R.E. Anderson, P.A. Batay-Csorba, D.A. Lind, H.H. Wieman, and C.D. Zafiratos, Nucl. Phys. **A293**, 83 (1977).